Short Communication

Acidification triggers Andes hantavirus membrane fusion and rearrangement of Gc into a stable post-fusion homotrimer

Rodrigo Acuña,[1] Eduardo A. Bignon,[1] Roberta Mancini,[2]
Pierre-Yves Lozach[3] and Nicole D. Tischler[1,4]

Correspondence
Nicole D. Tischler
ntischler@cienciavida.org

[1]Molecular Virology Laboratory, Fundación Ciencia & Vida, Av. Zanartu 1482, Santiago, Chile

[2]Institute of Biochemistry, ETH Zurich, Schafmattstrasse 18, 8093 Zurich, Switzerland

[3]Department of Infectious Diseases, Virology, University Hospital Heidelberg, Im Neuenheimer Feld 324, 69120 Heidelberg, Germany

[4]Facultad de Ciencias Biologicas, Universidad Andres Bello, República 275, Santiago, Chile

The hantavirus membrane fusion process is mediated by the Gc envelope glycoprotein from within endosomes. However, little is known about the specific mechanism that triggers Gc fusion activation, and its pre- and post-fusion conformations. We established cell-free *in vitro* systems to characterize hantavirus fusion activation. Low pH was sufficient to trigger the interaction of virus-like particles with liposomes. This interaction was dependent on a pre-fusion glycoprotein arrangement. Further, low pH induced Gc multimerization changes leading to non-reversible Gc homotrimers. These trimers were resistant to detergent, heat and protease digestion, suggesting characteristics of a stable post-fusion structure. No acid-dependent oligomerization rearrangement was detected for the trypsin-sensitive Gn envelope glycoprotein. Finally, acidification induced fusion of glycoprotein-expressing effector cells with non-susceptible CHO cells. Together, the data provide novel information on the Gc fusion trigger and its non-reversible activation involving lipid interaction, multimerization changes and membrane fusion which ultimately allow hantavirus entry into cells.

Hantaviruses are members of the family *Bunyaviridae* which bear tetrameric spike complexes consisting most likely of four Gn and four Gc envelope glycoproteins (Battisti *et al.*, 2011; Hepojoki *et al.*, 2010; Huiskonen *et al.*, 2010). How these glycoproteins mediate the entry of hantaviruses into cells is still largely unknown. After binding of glycoproteins to receptors, hantaviruses are taken up by endocytosis (Jin *et al.*, 2002; Ramanathan & Jonsson, 2008). They enter into cells by fusion of the viral membrane with the endosomal membrane (reviewed by Cifuentes-Muñoz *et al.*, 2014). This process is mediated by the Gc protein which seems to share similarity with class II fusion proteins (Tischler *et al.*, 2005). Hantavirus fusion activity has been demonstrated by syncytia formation upon low pH treatment of Vero E6 cells expressing the viral Gn and Gc glycoproteins and viral receptors. In this cellular context, a pH of 5.9 was found to activate fusion of Andes virus (ANDV), whilst a pH of 6.3 was reported for Hantaan virus (Cifuentes-Muñoz *et al.*, 2011; Ogino

et al., 2004), most probably influencing the site of endosomal escape. A role for endosomal pH in ANDV cell entry has been confirmed by the use of the weak base ammonium chloride, which inhibits ANDV entry by raising the pH of endosomes (Barriga *et al.*, 2013). For the bunyavirus Rift Valley fever virus, it has been shown that low pH is enough to trigger Gc multimerization changes which seem to be mediated by protonation of specific histidines (de Boer *et al.*, 2012). However, acidification is not the only activator of fusion proteins; some require priming by receptor interaction, proteolytic cleavage, specific membrane compositions or a combination of such and other triggers (reviewed by White *et al.*, 2008). The hantavirus glycoproteins are primed by proteolytical processing, most likely whilst being translated as glycoprotein precursor (GPC) (Löber *et al.*, 2001). During the entry process, a role of cellular factors in glycoprotein priming by thiol-isothiomerases has been previously suggested (Strandin *et al.*, 2011). Once activated, viral fusion proteins expose an amphipathic fusion peptide that drives their insertion into the target membrane (Epand, 2003; Harter *et al.*, 1989). In addition, the fusion process can involve a rearrangement of the oligomerization state of fusion

One supplementary figure is available with the online Supplementary Material.

proteins (reviewed by Baquero *et al.*, 2013; Harrison, 2015; Kielian, 2014).

So far, no information is available about the hantavirus fusion trigger and glycoprotein oligomerizations during the fusion process. To gain novel insights into the fusion entry mechanism of hantaviruses, we assessed whether acidification triggers fusion of hantaviruses in *in vitro* systems in the absence of cellular factors, and characterized the multimeric Gn and Gc rearrangements during the fusion process.

Towards this goal, fusion activation was assayed in terms of the binding of viral particles to membranes. Therefore, a liposome-based coflotation assay using large unilaminar vesicles (LUVs) was established through a sucrose step-gradient centrifugation. To reach the differential localization of LUVs and virus, the gradient was adjusted to 5, 15 and 25 % (w/v) as previously established for other enveloped viruses of similar size and density (Fritz *et al.*, 2008). Purified virus-like particles (VLPs) were used instead of infectious ANDV, which auto-assemble when the virus glycoproteins are being expressed (Acuña *et al.*, 2014). These VLPs contain a lipid envelope, expose grid-like glycoprotein protrusions and have a buoyant density of ~1.15 g ml^{-1} coinciding with that of hantaviruses (McCormick *et al.*, 1982; Schmaljohn *et al.*, 1983; White *et al.*, 1982). LUVs (200 nm) were prepared from phosphatidylcholine, phosphatidylethanolamine, sphingomyelin

and cholesterol (1 : 1 : 1 : 1.5) as described previously for fusion peptide insertion (Tischler *et al.*, 2005). For the detection of LUVs, the fluorescent probe 1,6-diphenyl-1,3,5-hexatriene (DPH) was incorporated. DPH (200 mM)-labelled LUVs were mixed with VLPs before or after their incubation for 30 min at the indicated pH. Next, the VLP/LUV mixture was added to the bottom of a step gradient and centrifuged for 2 h at 303 258 **g**. LUVs were detected by the fluorescence emission of DPH (excitation 230 nm; emission 320 nm) and VLPs by slot blot using anti-Gc mAb 5D11/G7 (Cifuentes-Muñoz *et al.*, 2011). When the VLP/liposome mixture was treated at neutral pH, the viral Gc protein was found exclusively in the bottom fractions of the gradient (Fig. 1a, fractions 1–3), whilst the liposomes were located only at the top (Fig. 1a, fractions 16–18). In contrast, after pH adjustment to 5.5, Gc was detected together with the liposomes in the uppermost fractions (Fig. 1b, upper slot blot), indicating VLP coflotation with liposomes. If, however, the liposomes were added after the low-pH incubation of VLPs, the VLPs stayed in the bottom fraction of the gradient (Fig. 1b, lower slot blot). Together, these results indicate acid-dependent interaction of VLPs with liposomes which further required that the viral glycoproteins were not pre-exposed to low pH. To confirm that direct contact may occur between VLPs and liposomes upon acidification, VLPs were mixed with multilaminar vesicles (MLVs), incubated at different pHs and analysed by negative-stain electron microscopy.
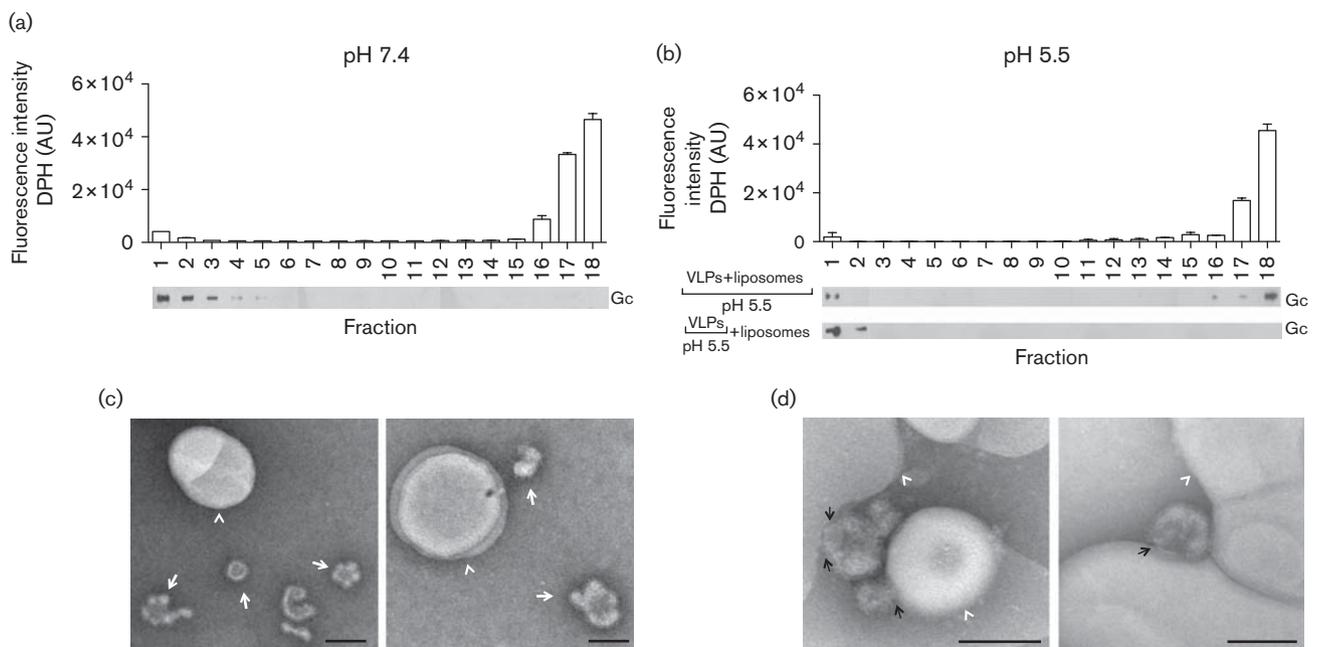
Fig. 1. Acid-induced target membrane interaction. (a, b) Coflotation assay of VLPs incubated with DPH-labelled LUVs at neutral pH (a) or VLPs incubated at pH 5.5 in the presence or absence of DPH-labelled LUVs (b). DPH fluorescence in (b) is representative of both conditions (*n*=3 experiments). AU, arbitrary units. (c, d) Representative negative-stain electron microscope images using phosphotungstic acid of unfixed ANDV VLPs incubated in the presence of MLVs at pH 7 (c) or 5.5 (d). White arrows, VLPs; white arrowheads, liposomes; black arrows, VLP/liposome interaction. Bar, 100 nm.

(a)

(b)

(c)

Formaldehyde	–	+	+
pH 5.5	–	+	–
pH 7.4	+	–	+

(d)
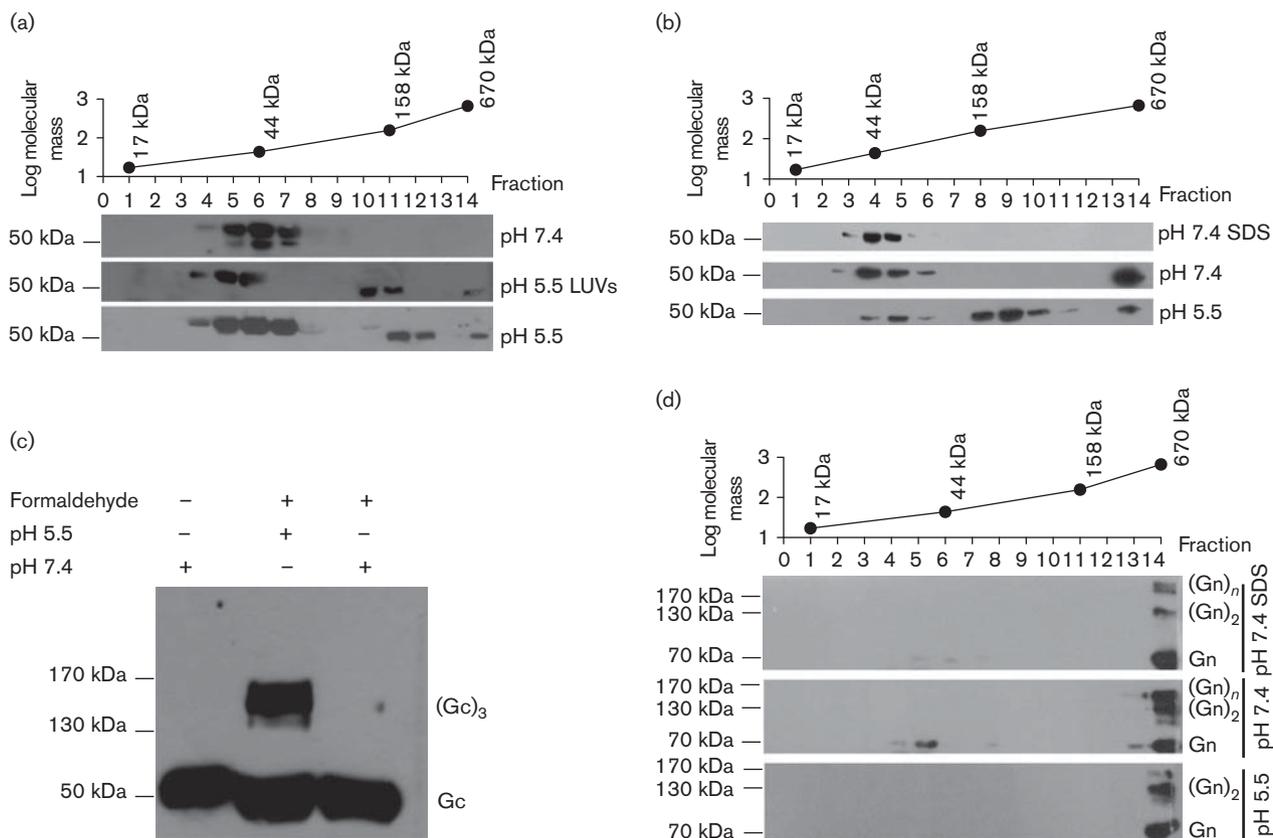
Fig. 2. (a–d) Acid-induced Gc homotrimer formation. Sucrose gradient sedimentation of ANDV (a) or VLPs (b, d) after their incubation at the indicated pHs in the presence or absence of LUVs. The molecular mass of each fraction was determined experimentally by a molecular marker and plotted against the log of its theoretical molecular mass. (c) Cross-linking of VLPs treated at different pHs and Western blot analysis. All results represent $n=3$ experiments.

The co-incubation of VLPs and liposomes at pH 5.5 allowed the observation of VLPs attached to membranes, whilst this was not the case at neutral pH (Fig. 1c, d). From these results it can be concluded that low pH is sufficient to trigger the interaction of ANDV glycoproteins with membranes in the absence of additional cellular factors.

In order to test if acidification induces not only target membrane insertion, but also a rearrangement of the viral glycoproteins, their multimerization states were assessed at different pHs by sucrose gradient centrifugation, as reported previously (Fritz et al., 2008). To this end, ANDV strain CHI-7913 (Galeno et al., 2002) was mixed with liposomes and incubated at 37 °C at the indicated pHs to allow multimerization changes. Subsequently, the glycoproteins were extracted from the lipid envelope by Triton X-100 0.5 % (v/v) and were added to the top of a gradient consisting of 7–15 % (w/v) sucrose. After 16 h of centrifugation at 148 596 g, fractions were collected, and the presence of Gn and Gc was analysed by Western blot using mAbs to anti-Gc and anti-Gn 6B9/F5 (Cifuentes-Muñoz et al., 2010). Gradient sedimentation of glycoproteins at neutral pH led to

the detection of Gc in fractions 4–7, including a maximum in fraction 6, coinciding with the expected molecular mass for Gc monomers of ~50 kDa (Fig. 2a, pH 7.4). In the reducing electrophoretic separation, two Gc migration bands were detected, which correspond probably to oxidized and reduced forms of Gc described previously (Hepojoki et al., 2010). When the ANDV/liposome mixture was treated at low pH, a new Gc population could be observed at ~150 kDa (fractions 10–11). From the molecular mass, it seems likely that this acid-induced Gc population corresponds to Gc trimers (Fig. 2a, pH 5.5 LUVs). No increase of the amount of Gc trimers was observed when ANDV was incubated at pH <5.5 (data not shown). In the higher-molecular-mass fractions, only the lower molecular migration band of Gc was observed, suggesting that Gc disulfide bridges were not accessible to reduction. The low-pH-induced Gc population was also observed when ANDV was acidified in the absence of liposomes (Fig. 2a, pH 5.5). The fact that Gc trimerization can occur in the absence of lipids, in line with previous studies, demonstrates that conformational changes occurring during fusion do not require
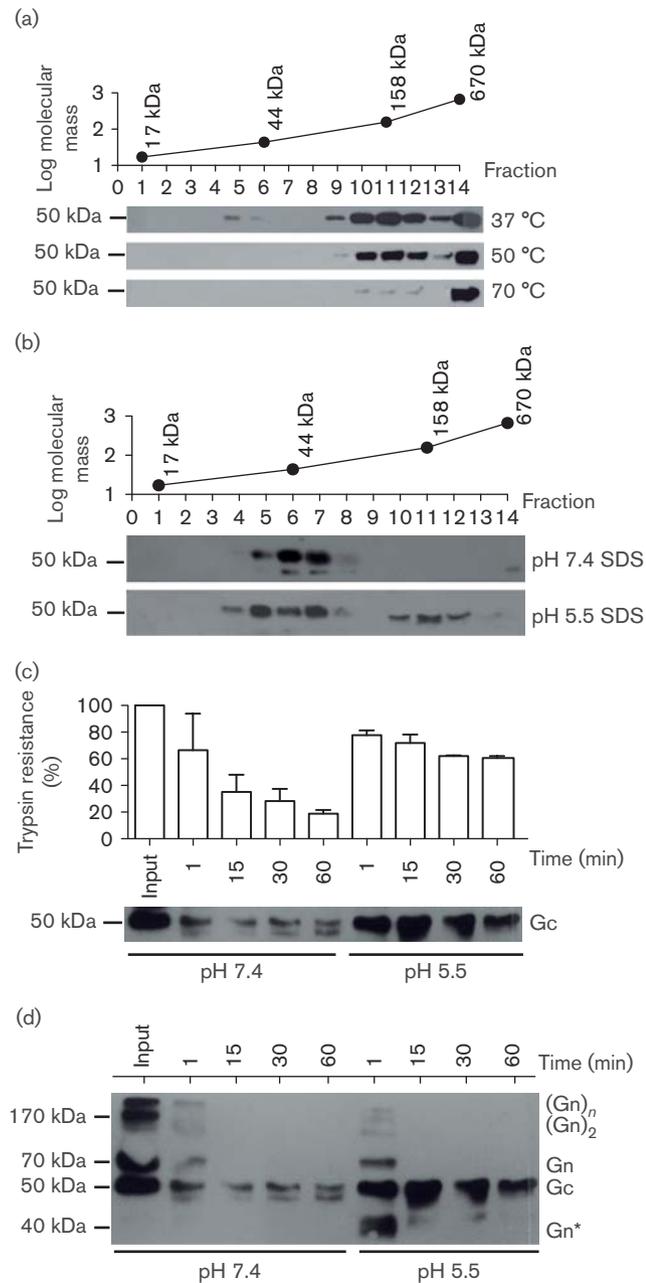
Fig. 3. Gc post-fusion homotrimer stability. (a, b) Sucrose gradient sedimentation after treatment of VLPs at low pH and subsequent incubation at different temperatures (a) or after treatment of ANDV at different pHs and subsequent incubation with 1 % (w/v) SDS (b). (c, d) Trypsin digestion of VLPs after neutral or low pH treatment and Western blot analysis with anti-Gc (c) or anti-Gc and anti-Gn antibodies (d) ($n=3$ experiments). The amount of Gc was quantified by densitometry ($n=3$) (ImageJ; Schneider et al., 2012). *, Digestion products.

fusion peptide insertion into a target membrane (Gibbons & Kielian, 2002).

We next analysed whether the VLP system for ANDV would undergo the same acid-triggered glycoprotein

rearrangement as the virus. VLPs treated at neutral pH led to the detection of Gc monomers of ~50 kDa (Fig. 2b, pH 7). At the bottom of the gradient, some Gc aggregates were detected, which disappeared when VLPs were incubated with 1 % (w/v) SDS prior to their application to the gradient (Fig. 2b, pH 7 SDS). When VLPs were incubated at pH 5.5, a new population of Gc oligomers with a molecular mass of ~150 kDa (fractions 8–10) was detected, corresponding most likely to Gc trimers in accordance with the results obtained for ANDV.

The ratio of Gc trimers to monomers was always higher when Gc was derived from VLPs than from ANDV (Fig. 2a, b, condition pH 5.5). This difference may be related to the higher purity of the VLP preparation compared with that of the virus.

The molecular mass of the low-pH-induced Gc trimers was further corroborated by an alternative strategy, involving the cross-linking of glycoproteins by 2 % (v/v) formaldehyde. When VLPs at neutral pH were cross-linked, a single band migrating at ~50 kDa was observed for Gc, matching the mass of monomeric Gc from the untreated control (Fig. 2c, lanes 1 and 3). In comparison, when VLPs were acidified and subsequently cross-linked, a new band with a molecular mass of ~150 kDa was detected (Fig. 2c, lane 2), coinciding with the results for the molecular mass of acid-induced Gc oligomers observed by sucrose gradient centrifugation using ANDV and VLPs (Fig. 2a, b). Taking into account the molecular mass of ~70 kDa for Gn, the molecular mass of the low-pH-induced Gc oligomers determined by both experimental approaches suggests that an arrangement of Gc into homotrimers would match best with this size.

To discard the participation of Gn in this low-pH-induced Gc trimer arrangement and to gain insights into the multimerization of Gn during viral cell entry, the molecular states of Gn were analysed. Most Gn was found in oligomeric assemblies at the bottom of the gradient, independent of the applied pHs (Fig. 2d). This result coincides well with previous results for the Tula hantavirus Gn at neutral pH that demonstrate homo-oligomerization of Gn (Hepojoki et al., 2010). However, based on the resolution of the sucrose gradient, changes in the arrangements of higher oligomeric Gn associations cannot be excluded. These results were obtained with glycoproteins extracted either from VLPs (Fig. 2d) or ANDV (data not shown) and allow for the conclusion that Gn does not participate in a heteromeric interaction with the low-pH-induced Gc oligomers. Therefore, the data strongly suggest that the acid-triggered Gc oligomers of ~150 kDa, which were detected by sucrose sedimentation and cross-linking, correspond to Gc homotrimers.

In general, viral fusion proteins are assembled into multimeric associations in a metastable pre-fusion conformation and homotrimerize upon fusion activation (reviewed by Harrison, 2015). The final post-fusion conformation of all the viral fusion proteins that have been characterized

so far corresponds to a trimer of hairpins (Kielian & Rey, 2006), which in the case of class I and class II fusion proteins form highly stable non-reversible structures (Gibbons & Kielian, 2002; Gibbons et al., 2000; Kielian et al., 2010; Skehel & Wiley, 1998). In this context, the reversibility of Gc trimerization was assayed. The sucrose sedimentation of acidified VLPs or acidified and back-neutralized VLPs showed that the pH after the acidification did not influence the amount of Gc homotrimers (data not shown). This observation coincides with the coflotation results showing that glycoproteins must be present in their pre-fusion conformation to allow their membrane interaction (Fig. 1b). Together, these data indicate that the low-pH-induced Gc fusion activation was not reversible. To further examine if the acid-induced Gc homotrimers shared features with a highly stable post-fusion arrangement, their resistance to temperature, detergent and proteolytic cleavage was examined. For the thermostability analysis, VLPs were treated at pH 5.5 and subsequently incubated at different temperatures. Sucrose gradient centrifugation revealed the stability of Gc homotrimers up to 50 °C. However, heating acidified VLPs to 70 °C led to the aggregation of Gc (Fig. 3a). Next, the resistance to ionic detergent treatment was assayed by incubation of low-pH-treated ANDV with SDS. In the presence of SDS, the population of Gc homotrimers was readily detected by sucrose sedimentation, indicating that the homotrimers were also resistant to detergent (Fig. 3b). To further test if the trimerization of Gc may hide protease cleavage sites, VLPs treated at different pHs were incubated with trypsin. The neutral pH form of Gc was trypsin-sensitive, leading to a decrease in Gc within 15 min and almost complete digestion within 60 min (Fig. 3c). In contrast, the low pH conformation of Gc remained mostly resistant to trypsin during the same time frame (Fig. 3c). When the same Western blot membrane was further immunostained with anti-Gn mAb, a decreasing amount of Gn could be visualized under both pH conditions after 1 min of incubation and after 15 min Gn was no longer detectable (Fig. 3d).

The induction of a stable Gc homotrimer by low pH not only shows that acidification triggers fusion, but further suggests that complete fusion occurred. To corroborate this, a novel cell–cell fusion assay with non-susceptible CHO cells (Choi et al., 2008; Gavrilovskaya et al., 1998) based on Calcein AM (Molecular Probes) dequenching was adapted from Crowe et al. (1995) and Kendall & Mac-Donald (1982). The results show that 293FT cells that express ANDV GPC fuse with CHO cells, but not with non-transfected 293FT cells or 293FT cells that express the fusion-inactive mutant GPC (GcW115A) (Fig. S1, available in the online Supplementary Material).

Taken as a whole, the results presented here demonstrate that acidification triggers the fusion of hantaviruses and that Gc follows a non-reversible fusion process upon low pH exposure, leading to a stable post-fusion homotrimer. To the best of our knowledge, this work is the first report on a stable fusion protein homotrimer in the

family *Bunyaviridae* and adds new information about the cooperative function of hantavirus glycoproteins during viral cell entry. How the tetrameric spikes on hantaviruses rearrange during the fusion process to allow the assembly of Gc homotrimers has to be determined in future studies.

References

Acuña, R., Cifuentes-Muñoz, N., Márquez, C. L., Bulling, M., Klingström, J., Mancini, R., Lozach, P. Y. & Tischler, N. D. (2014). Hantavirus Gn and Gc glycoproteins self-assemble into virus-like particles. *J Virol* **88**, 2344–2348.

Baquero, E., Albertini, A. A., Vachette, P., Lepault, J., Bressanelli, S. & Gaudin, Y. (2013). Intermediate conformations during viral fusion glycoprotein structural transition. *Curr Opin Virol* **3**, 143–150.

Barriga, G. P., Martínez-Valdebenito, C., Galeno, H., Ferrés, M., Lozach, P. Y. & Tischler, N. D. (2013). A rapid method for infectivity titration of Andes hantavirus using flow cytometry. *J Virol Methods* **193**, 291–294.

Battisti, A. J., Chu, Y. K., Chipman, P. R., Kaufmann, B., Jonsson, C. B. & Rossmann, M. G. (2011). Structural studies of Hantaan virus. *J Virol* **85**, 835–841.

Choi, Y., Kwon, Y. C., Kim, S. I., Park, J. M., Lee, K. H. & Ahn, B. Y. (2008). A hantavirus causing hemorrhagic fever with renal syndrome requires gC1qR/p32 for efficient cell binding and infection. *Virology* **381**, 178–183.

Cifuentes-Muñoz, N., Darlix, J. L. & Tischler, N. D. (2010). Development of a lentiviral vector system to study the role of the Andes virus glycoproteins. *Virus Res* **153**, 29–35.

Cifuentes-Muñoz, N., Barriga, G. P., Valenzuela, P. D. T. & Tischler, N. D. (2011). Aromatic and polar residues spanning the candidate fusion peptide of the Andes virus Gc protein are essential for membrane fusion and infection. *J Gen Virol* **92**, 552–563.

Cifuentes-Muñoz, N., Salazar-Quiroz, N. & Tischler, N. D. (2014). Hantavirus Gn and Gc envelope glycoproteins: key structural units for virus cell entry and virus assembly. *Viruses* **6**, 1801–1822.

Crowe, W. E., Altamirano, J., Huerto, L. & Alvarez-Leefmans, F. J. (1995). Volume changes in single N1E-115 neuroblastoma cells measured with a fluorescent probe. *Neuroscience* **69**, 283–296.

de Boer, S. M., Kortekaas, J., Spel, L., Rottier, P. J., Moormann, R. J. & Bosch, B. J. (2012). Acid-activated structural reorganization of the Rift Valley fever virus Gc fusion protein. *J Virol* **86**, 13642–13652.

Epand, R. M. (2003). Fusion peptides and the mechanism of viral fusion. *Biochim Biophys Acta* **1614**, 116–121.

Fritz, R., Stiasny, K. & Heinz, F. X. (2008). Identification of specific histidines as pH sensors in flavivirus membrane fusion. *J Cell Biol* **183**, 353–361.

Galeno, H., Mora, J., Villagra, E., Fernandez, J., Hernandez, J., Mertz, G. J. & Ramirez, E. (2002). First human isolate of Hantavirus (Andes virus) in the Americas. *Emerg Infect Dis* **8**, 657–661.

Gavrilovskaya, I. N., Shepley, M., Shaw, R., Ginsberg, M. H. & Mackow, E. R. (1998). Beta$_3$ Integrins mediate the cellular entry of hantaviruses that cause respiratory failure. *Proc Natl Acad Sci U S A* **95**, 7074–7079.

Gibbons, D. L. & Kielian, M. (2002). Molecular dissection of the Semliki Forest virus homotrimer reveals two functionally distinct regions of the fusion protein. *J Virol* **76**, 1194–1205.

Gibbons, D. L., Ahn, A., Chatterjee, P. K. & Kielian, M. (2000). Formation and characterization of the trimeric form of the fusion protein of Semliki Forest Virus. *J Virol* **74**, 7772–7780.

Harrison, S. C. (2015). Viral membrane fusion. *Virology* **479-480**, 498–507.

Harter, C., James, P., Bächi, T., Semenza, G. & Brunner, J. (1989). Hydrophobic binding of the ectodomain of influenza hemagglutinin to membranes occurs through the ''fusion peptide''. *J Biol Chem* **264**, 6459–6464.

Hepojoki, J., Strandin, T., Vaheri, A. & Lankinen, H. (2010). Interactions and oligomerization of hantavirus glycoproteins. *J Virol* **84**, 227–242.

Huiskonen, J. T., Hepojoki, J., Laurinmäki, P., Vaheri, A., Lankinen, H., Butcher, S. J. & Grünewald, K. (2010). Electron cryotomography of Tula hantavirus suggests a unique assembly paradigm for enveloped viruses. *J Virol* **84**, 4889–4897.

Jin, M., Park, J., Lee, S., Park, B., Shin, J., Song, K. J., Ahn, T. I., Hwang, S. Y., Ahn, B. Y. & Ahn, K. (2002). Hantaan virus enters cells by clathrin-dependent receptor-mediated endocytosis. *Virology* **294**, 60–69.

Kendall, D. A. & MacDonald, R. C. (1982). A fluorescence assay to monitor vesicle fusion and lysis. *J Biol Chem* **257**, 13892–13895.

Kielian, M. (2014). Mechanisms of virus membrane fusion proteins. *Annu Rev Virol* **1**, 171–189.

Kielian, M. & Rey, F. A. (2006). Virus membrane-fusion proteins: more than one way to make a hairpin. *Nat Rev Microbiol* **4**, 67–76.

Kielian, M., Chanel-Vos, C. & Liao, M. (2010). Alphavirus entry and membrane fusion. *Viruses* **2**, 796–825.

Löber, C., Anheier, B., Lindow, S., Klenk, H. D. & Feldmann, H. (2001). The Hantaan virus glycoprotein precursor is cleaved at the conserved pentapeptide WAASA. *Virology* **289**, 224–229.

McCormick, J. B., Palmer, E. L., Sasso, D. R. & Kiley, M. P. (1982). Morphological identification of the agent of Korean haemorrhagic fever (Hantaan virus) as a member of the *Bunyaviridae*. *Lancet* **319**, 765–768.

Ogino, M., Yoshimatsu, K., Ebihara, H., Araki, K., Lee, B. H., Okumura, M. & Arikawa, J. (2004). Cell fusion activities of Hantaan virus envelope glycoproteins. *J Virol* **78**, 10776–10782.

Ramanathan, H. N. & Jonsson, C. B. (2008). New and Old World hantaviruses differentially utilize host cytoskeletal components during their life cycles. *Virology* **374**, 138–150.

Schmaljohn, C. S., Hasty, S. E., Harrison, S. A. & Dalrymple, J. M. (1983). Characterization of Hantaan virions, the prototype virus of hemorrhagic fever with renal syndrome. *J Infect Dis* **148**, 1005–1012.

Schneider, C. A., Rasband, W. S. & Eliceiri, K. W. (2012). NIH Image to ImageJ: 25 years of image analysis. *Nat Methods* **9**, 671–675.

Skehel, J. J. & Wiley, D. C. (1998). Coiled coils in both intracellular vesicle and viral membrane fusion. *Cell* **95**, 871–874.

Strandin, T., Hepojoki, J., Wang, H., Vaheri, A. & Lankinen, H. (2011). Inactivation of hantaviruses by *N*-ethylmaleimide preserves virion integrity. *J Gen Virol* **92**, 1189–1198.

Tischler, N. D., Gonzalez, A., Perez-Acle, T., Rosemblatt, M. & Valenzuela, P. D. (2005). Hantavirus Gc glycoprotein: evidence for a class II fusion protein. *J Gen Virol* **86**, 2937–2947.

White, J. D., Shirey, F. G., French, G. R., Huggins, J. W., Brand, O. M. & Lee, H. W. (1982). Hantaan virus, aetiological agent of Korean haemorrhagic fever, has *Bunyaviridae*-like morphology. *Lancet* **319**, 768–771.

White, J. M., Delos, S. E., Brecher, M. & Schornberg, K. (2008). Structures and mechanisms of viral membrane fusion proteins: multiple variations on a common theme. *Crit Rev Biochem Mol Biol* **43**, 189–219.